Effect of impurity scattering on the linear and nonlinear conductances of quasi-one-dimensional disordered quantum wires by asymmetrically lateral confinement

2010 J. Phys.: Condens. Matter 22 395303

(http://iopscience.iop.org/0953-8984/22/39/395303)

J. Phys.: Condens. Matter **22** (2010) 395303 (7pp) doi:10.1088/0953-8984/22/39/395303

Effect of impurity scattering on the linear and nonlinear conductances of quasi-one-dimensional disordered quantum wires by asymmetrically lateral confinement

K M Liu[1], C H Juang[1], V Umansky[2] and S Y Hsu[1]

[1] Department of Electrophysics, National Chiao Tung University, Hsinchu 30010, Taiwan
[2] Braun Center for Submicron Research, Weizmann Institute of Science, Rehovot 76100, Israel

E-mail: syhsu@mail.nctu.edu.tw

Received 4 June 2010, in final form 23 August 2010
Published 10 September 2010
Online at stacks.iop.org/JPhysCM/22/395303

Abstract

We have studied the linear conductance and source–drain bias spectroscopies of clean and disordered quantum wires (QWs) against thermal cycling and lateral shifting, which change the impurity configuration. Conductance quantization and the zero bias anomaly (ZBA) are robust in clean QWs. In contrast, disordered QWs show complexities in the ways of conductance resonance, peak splitting and trace crossing in source–drain bias spectroscopies. The experimental results and theoretical predictions are in congruence. Moreover, the resonant state arising from the impurities results in either a single peak or double-splitting peaks in the spectroscopies from the detailed impurity configurations. The resonant splitting peaks are found to influence the ZBA, indicating that a clean QW is crucial for investigating the intrinsic characteristics of the ZBA of QWs.

(Some figures in this article are in colour only in the electronic version)

1. Introduction

In a ballistic quasi-one-dimensional (1D) channel the linear conductance is quantized in integer multiples of $G_o = 2e^2/h$ due to the transmission of spin-degenerate 1D subbands within a noninteracting electron picture [1, 2]. However, it has been well known that impurities in a nearly perfect conductor backscatter the incident electron wave and degrade the conductance quantization [3–6]. The study of transport in the presence of impurities is important, since physical devices are usually not free of an impurity [7]. Moreover, lattice defects, randomly distributed ionized donors or edge roughness can make a quantum wire (QW) disordered. From theoretical points of view, the impurities bring about quasi-bound states giving rise to conductance oscillations [4, 8–13] and offsetting the pinch-off voltage as a result of the addition of resonant levels [3, 13, 14]. In previous experiments, the linear conductance resonances in unintentionally disordered QWs were attributed to one single impurity [8], interface roughness [15], random potential fluctuations [16, 17] and length resonances [18]. However, experimental observations directly associated with the aforementioned predictions are still scarce.

In this work, we present comparisons of linear conductance and source–drain bias spectroscopy between clean and disordered QWs. We particularly adopted a lateral shifting technique to systematically vary the impurity configurations in disordered QWs. Laterally shifting the QWs by independently biasing the split gate voltage implies spatial displacement of the confined 1D channel with an asymmetrically confining potential, which was supported by theoretical calculations [19, 20]. This technique has been widely used in experimental studies of random telegraph noises in QWs [21–23]. The characteristics of the noises relate to the relative location of deep center defects, suggesting that the impurity configuration was modified corresponding to

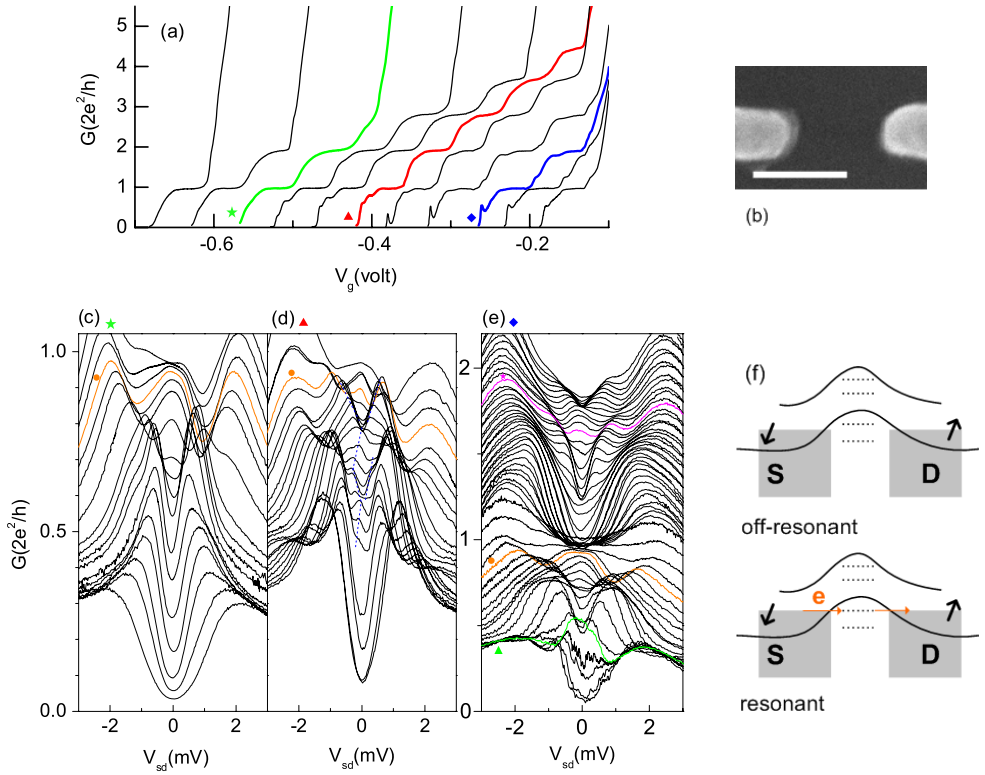

Figure 1. (a) $G(V_g)$ against $\Delta\tilde{V}_g$ of a disordered QW in the presence of strong conductance oscillations at 0.3 K. $\Delta\tilde{V}_g = +0.5$ (leftmost) ~ -0.5 V (rightmost) in 0.1 V steps. (b) Micrograph of the disordered QW. The scale bar has a length of 0.4 μm. (c)–(e) Source–drain bias spectroscopies for various $\Delta\tilde{V}_g$. (c) +0.3 V, (d) 0 V and (e) −0.3 V. Dashed lines are visual guides for the evolution of conductance peaks as a function of V_g and V_{sd}. (f) Scenario for the splitting peaks in source–drain bias spectroscopies. The thick lines stand for the last two subbands of a QW while the dotted lines stand for the resonant levels induced by impurities.

the QW displacement. Here, we show that the conductance quantization and the zero bias anomaly (ZBA), referred to as the conductance peak centered at zero bias in source–drain bias spectroscopies, are robust against thermal cycling and lateral shifting of the QWs in clean QWs. In contrary, the conductance plateaus are distorted and superimposed with resonances in disordered QWs. The fine features of spectroscopies vary correspondingly to the impurity configurations. The nonlinear conductance traces demonstrate splitting peaks which evolve with the gate voltage and resolve back into a single peak. This feature may be confusing with the inherent ZBA of QWs. Moreover, trace crossing, triple-peak structure and additional fine structures are also observable at higher subbands in the spectroscopies. The results indicate that the ZBA is an inherent feature of QWs; nevertheless, cleanness is critical for investigating its genuine characteristics.

2. Experiments

The two-dimensional electron gas (2DEG) that forms at the interface of a GaAs/$Al_xGa_{1-x}As$ heterostructure was grown using molecular beam epitaxy at the Weizmann Institute in Israel. Shubnikov–de Haas and Hall measurements were used to determine the areal electron density n. Mobility is approximately 1.7×10^6 cm^2 V^{-1} s^{-1} and n is 2.4×10^{11} cm^{-2}, corresponding to the elastic mean free path ℓ_e of $\sim$14 μm at low temperatures. Electron beam lithography along with thermal deposition was used to fabricate metallic gates on the (100) plane of the substrate. Measurements were performed in a pumped ^{3}He cryostat with a base temperature of 0.27 K. All presented data were taken at 0.3 K. Differential conductance was carried out by standard four-terminal ac lock-in technique at 51 Hz, with a small excitation voltage of 10 μV.

The QW is created by negatively biasing a pair of split gates, depleting the 2DEG $\sim$93 nm beneath the surface. The lithographic gap distance between both gates is about 0.45 μm, while the length of QWs covers quasi-zero, 0.2, and 0.5 μm. To control the position of the QWs and impose various impurity configurations, the split gates were offset by a voltage bias, ΔV_g. Without being mentioned throughout the paper, $V_g+\frac{1}{2}\Delta V_g$ was applied on one gate and $V_g-\frac{1}{2}\Delta V_g$ was applied on the other. The position displacement is linearly dependent with ΔV_g [19, 20]. Unlike the devices affected by deep center defects in other reports, the results here show no random telegraph noise. For comparison, results of a 0.3 μm QW, intentionally disordered by imposing a small local widening, and a clean quasi-zero-length QW were studied as well. The presented results are typical features based on measurements of ten disordered and three clean short QWs.

3. Results and discussion

When both split gates are applied to the same negative voltage, the confining potential of the QW is transversely symmetric and the transport is a typically quantized conductance behavior. The middle red line labeled by a triangle shown in figure 1(a)

is an example of this case. However, weak conductance oscillations are discernible along the conductance trace besides the five conductance plateaus. By differentially biasing both gates by $\Delta\tilde{V}_g$, V_g being applied on one gate (right) and $V_g + \Delta\tilde{V}_g$ being applied on the other gate (left), the confining potential becomes asymmetric and conductance traces evolve differently. Figure 1(b) displays the scanning electron microscopic (SEM) image of both gates. In figure 1(a) we also plot other conductance traces against a series of $\Delta\tilde{V}_g$, from +0.5 to −0.5 V in 0.1 V steps. The QW is monotonically shifted with $\Delta\tilde{V}_g$. The pinch-off voltage decreases (becomes more negative) with increasing $\Delta\tilde{V}_g$. The electron path is shifted slightly towards the right for a negative $\Delta\tilde{V}_g$ while it shifts to the left for a positive $\Delta\tilde{V}_g$. As seen in figure 1(a), the number of plateaus is reduced by the asymmetrical confining potential. The confining potential is higher and steeper for the more negatively biased gate while being lower and smoother for the other less negatively biased gate. A strong resonant peak emerges by shifting the QW to the right (lowering the confining potential at the right-hand side) for $\Delta\tilde{V}_g \leqslant -0.1$ V, while the peak conductance tends to pin at $0.5G_o$. Notice that the superimposing resonances are stronger for the negative $\Delta\tilde{V}_g$ regime.

The source–drain bias spectroscopy was investigated by sweeping a dc source–drain voltage V_{sd} across a confined QW and measuring the dynamic conductance $G = \mathrm{d}I/\mathrm{d}V_{sd}$. The effect of the resonances on the source–drain bias spectroscopy is presented in figures 1(c)–(e) for three $\Delta\tilde{V}_g$. The ZBA, conductance peak at $V_{sd} = 0$, is seen in all three spectroscopies for $G < G_o$ coexisting with the splitting peaks at nonzero V_{sd}. For instance, two strong satellite peaks appear at the sides of the ZBA at $|V_{sd}| \sim 0.8$ mV on the dot-labeled curve of $V_g = -383$ mV in figure 1(d). Similar phenomena have been reported by Sfigakis *et al* for dot-coupled QWs [24]. The concurrence of the ZBA and resonant peaks forming a triple-peak structure can be attributed to the resonant states. The characteristics of the ZBA, i.e. the amplitude and width of the conductance peak, are affected by the resonant peaks. The satellite peaks appear at larger $|V_{sd}|$ for an asymmetric confining potential, e.g. at ∼1.9 mV in figure 1(c) of $\Delta\tilde{V}_g = +0.3$ V, and at ∼1.8 mV in figure 1(e) of $\Delta\tilde{V}_g = -0.3$ V for the dot-labeled curves. Compared with figures 1(c) and (e), the ZBA is weaker and suppressed more rapidly with decreasing V_g for a symmetric confining potential ($\Delta\tilde{V}_g = 0$) as shown in figure 1(d). The results indicate that the existence of the resonant peaks due to the resonant states near the $V_{sd} = 0$ suppresses the ZBA. The evolution of the split peaks with respect to V_g, indicated by the dashed lines in figure 1(d), resembles the diamond structure of the tunneling spectroscopy of zero-dimensional states. A similar evolution of the satellite peaks is also observable in figure 1(e) in both conductance ranges, $G < G_o$ and $G_o < G < 1.75G_o$, for the higher subband.

The triple-peak structure appears also at the higher conductance regime for $1.55G_o < G < 1.75G_o$ at $\Delta\tilde{V}_g = -0.3$ V as shown in figure 1(e). The central peak in this range is weaker compared with the strong *single* peak observed in the same conductance range in the clean QW (see the following paragraphs). The appearance of the central peak at such a high conductance regime implies that the ZBA is not unique for the low conductance regime on which most research groups focused. Although there is no resonance in the linear conductance trace for $\Delta\tilde{V}_g = +0.3$ V, groups of crossed traces appear in all three graphs, indicating strong conductance resonances in the finite V_{sd} regime. Available levels of a QW in the presence of resonant states induced by impurities are depicted in figure 1(f). Thick and dotted lines represent the last two subbands and impurity-induced resonant levels, respectively. Alignment of a resonant level with the chemical potential of either source or drain increases the transmission probability or the differential conductance G. The mechanism is analogous to the resonant tunneling in a quantum dot. Finite V_{sd} would be required to align the chemical potential with a resonant state when the QW is not initially in resonance, resulting in the evolution of splitting peaks with respect to V_g in spectroscopy and conductance resonances at finite V_{sd}. Although this is an oversimplified scenario, it provides a qualitatively suitable explanation for our results. Additionally, when the QW is shifted by $\Delta\tilde{V}_g$, the relative position of the impurity is changed as well as the details of the resonant state. As expected, figures 1(c)–(e) present different curve structures for these three $\Delta\tilde{V}_g$.

For comparison, the linear conductance of a clean QW of quasi-zero length (figure 2(a)) in two separate cooling processes is shown in figures 2(b) and (c). Both traces reveal non-oscillating conductance and clear quantization steps without distortions, implying that the sample is less disordered. The plateaus can be aligned exactly to integer multiples of G_o by subtracting a series resistance of about 300 Ω from the data, such as in [25] by Thomas *et al*. We present the raw data here since the series resistance does not affect our results. Figure 2(d) shows the spectroscopy in the first cooling operation. The nonlinear dynamic conductance exhibits clearly a series of single peaks centered at $V_{sd} = 0$ for $G < G_o$, referred to as ZBA. The ZBA is reproducible after thermal cycling, as shown in figure 2(e) for the second cooling process. Notice that the half-plateaus and the 0.7 anomaly at finite biases are visible as bunches of curves (as opposed to crossing traces due to resonant states) at $G \sim 1.5G_o$ and $G \sim 0.8G_o$ for $V_{sd} > 1.4$ mV and $V_{sd} > 0.7$ mV, respectively.

Since 2DEG is generally not free of disorder [7], lateral shifting was exploited to further scrutinize the quality of the sample. To avoid the QW width being predominately affected by lateral shifting (ΔV_g), we adopted the bias configuration mentioned in the previous section for the split gates. Figure 3(a) shows conductance traces against a series of ΔV_g. The traces are offset in turn in 50 mV steps for clarity. At $\Delta V_g = 0$, the conductance trace demonstrates more than 14 clear quantization steps. Since the pinch-off voltage remains the same, being independent of ΔV_g, the plotted traces are certainly uniformly spaced at 50 mV spacing for the artificial offset. A slight conductance oscillation appears at the sixth and seventh steps for $\Delta V_g = +0.2$ and +0.4 V. Except for this small disturbance, the conductance quantization remains unaltered with respect to the lateral shifting, confirming that the device is quite clean. Figures 3(b)

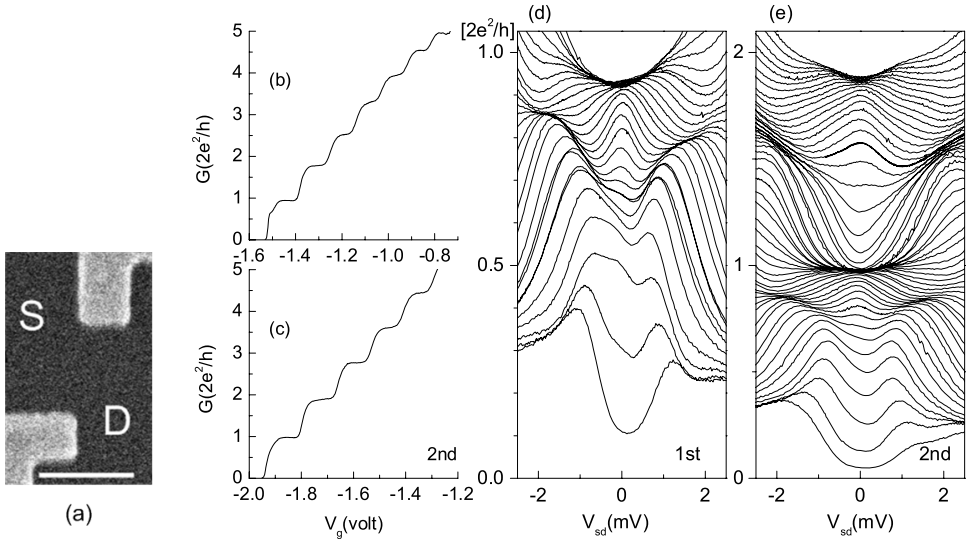

Figure 2. (a) Micrograph of a clean QW with a length of quasi-zero. The white scale bar indicates a length of 0.5 μm. (b)–(c) Zero bias differential conductance G versus split gate voltage V_g. (d)–(e) Source–drain bias spectroscopies in two separate cooldowns at 0.3 K of the clean quantum wire. Traces of $G(V_{sd})$ are for discrete consequential split-gate voltages in 4 mV steps. (d) $V_g = -1.450 \sim -1.558$ V. (Top to bottom) (e) $V_g = -1.720 \sim -1.944$ V.

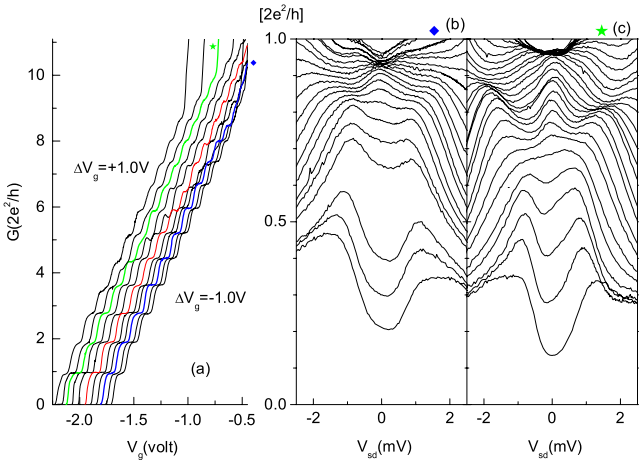

Figure 3. (a) $G(V_g)$ of the clean quantum wire against the differential voltage difference ΔV_g. (See text) From left to right, $\Delta V_g = +1.0 \sim -1.0$ V in 0.2 V steps. The traces are offset in turn by 50 mV for clarity. The middle red line is for $\Delta V_g = 0$. (b)–(c) Source–drain bias spectroscopies for $\Delta V_g = -0.6$ and $+0.6$ V, respectively. (b) $V_g = -1.846 \sim -1.934$ V in 4 mV steps. (c) $V_g = -1.848 \sim -1.964$ V in 4 mV steps.

and (c) show the spectroscopies of the QW at two opposite conditions, $\Delta V_g = +0.6$ and -0.6 V. The QW is shifted from one side to the other relative to the symmetrical confinement at $\Delta V_g = 0$. Both figures demonstrate ZBA for $G < G_o$. The ZBA is slightly weaker in figure 3(b). However, there is no additional structure such as satellite peaks compared with the disordered QWs in figure 1. The varying ZBA characteristics are understandable. It has been known that the characteristics of the ZBA is sensitive to electron scattering, which is affected by local electric fields, electron density or physical geometry of a device [26]. For a pair of ideally symmetrical split gates, one would expect the ZBA to be identical for these two ΔV_g. The slight differences between these two series may be due to the minor asymmetry of the realistic gate edge and the random potential fluctuations due to ionized donors [17], which is beyond the experimental resolution. Nevertheless, the ZBA is a rather robust feature of low disordered QWs. Furthermore, neither peak splitting nor trace crossing is observed in their spectroscopies of clean QWs confined by asymmetrical potentials.

To carry out further examinations, the results of two unintentionally disordered QWs are displayed in figure 4. As seen in figure 4(a), the SEM image shows three devices that are close to each other. Although with the long ℓ_e of the bulk 2DEG, devices with long split-gate lengths of several micrometers fabricated closely in parallel are disordered. The impurities are suspected to arise from the damage to the 2DEG due to locally concentrated backscattered electrons with high energies during the pattern transferring in e-beam lithography. Figures 4(b) and (c) show the linear conductance of two short QWs (A and B). Traces of $G(V_g)$ are plotted against the lateral shifting voltage ΔV_g and are also offset in turn in 50 mV steps for clarity. The plateau conductances are much lower than the expected integer multiples of G_o in both devices, implying that the electrons are backscattered. Therefore, more steps are present in a smaller conductance range. For instance, more than eight steps are visible in the range of $0 < G < 5G_o$ on the $\Delta V_g = 0$ trace for sample A in figure 4(b). The higher subband conductance shows slight distortions. Sample B is much more disordered with more missing plateaus and lower conductance. One thing worth being noticed is that the traces are expected to be uniformly spaced if the subband energies remain unchanged with respect to the displacement of the QW, i.e. the pinch-off voltage is unchanged. However, in both figures, traces are closer to each other at the positive ΔV_g side but looser at the other. In a clean QW, the conductance traces are more

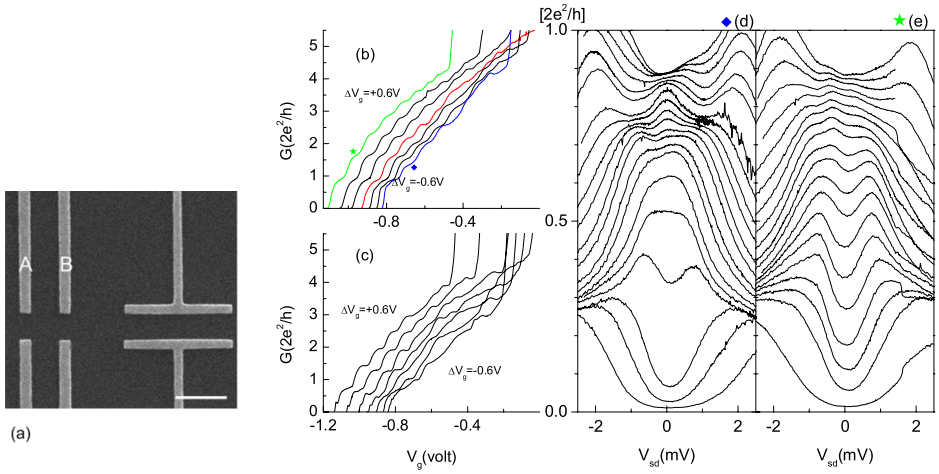

Figure 4. (a) Micrograph of the disordered QWs A and B. The white scale bar indicates a length of 1 μm. (b) Sample A. $G(V_g)$ versus the voltage difference ΔV_g. $\Delta V_g = +0.6$ (leftmost, labeled by a star) ~ -0.6 V (rightmost, labeled by a diamond) in 0.2 V steps. The traces are offset in turn by 50 mV. (c) Sample B. $G(V_g)$ versus ΔV_g for the same conditions. Traces are offset in 50 mV steps. (d)–(e) Source–drain bias spectroscopies of sample A with asymmetrically confining potential for two opposite ΔV_g. (d) $\Delta V_g = -0.6$ V. $V_g = -900 \sim -969$ mV in 3 mV steps. (e) $\Delta V_g = +0.6$ V. $V_g = -900 \sim -960$ in 3 mV steps.

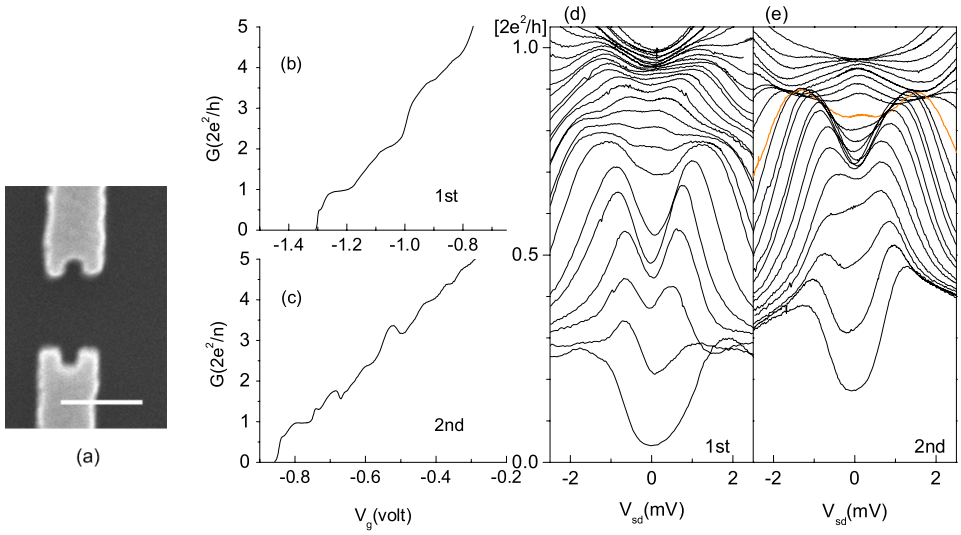

Figure 5. (a) Micrograph of a QW with a small local widening. The white scale bar indicates a length of 0.5 μm. (b)–(c) $G(V_g)$ and (d)–(e) source–drain bias spectroscopies in two separate cooldowns of the QW at 0.3 K. (d) $V_g = -1.140 \sim -1.248$ V in 4 mV steps. (e) $V_g = -0.780 \sim -0.845$ V in 3 mV steps.

uniformly spaced, referring to the previous discussion. The traces are much uniformly spaced in figure 3(a). This suggests that the threshold energies of subbands vary with the location of impurities, or effectively with the impurity configurations. In addition, a couple of conductance resonances are observed for $G < G_o$ for sample B in figure 4(c). The results are in congruence with the predictions that the quasi-bound state in a QW arisen from the impurities leads to conductance resonance and alters the subband threshold voltage [4, 9–13].

Figure 4(d) is the spectroscopy, $G(V_{sd})$ against a series of V_g, of sample A confined by an asymmetric potential for $\Delta V_g = -0.6$ V. It demonstrates a series of single peaks centered at $V_{sd} = 0$ for $G < G_o$, which resembles the ZBA of QWs. However, the single peak evolves into double-splitting peaks by shifting the QW to the other side at $\Delta V_g = +0.6$ V as shown in figure 4(e). The energy difference of the splitting, ϵ_d, is not a constant. ϵ_d decreases with decreasing V_g for $0.72G_o < G < G_o$ and begins to increase for $G \leqslant 0.72G_o$. The peak splitting is generally observed in disordered QWs and is believed not to be a feature of the ZBA of QWs [27, 28].

To further confirm the influence of impurities on the electrical transport in QWs, a 'stand-alone' pair of 0.3 μm split gates intentionally imposed with a disorder is also studied (as opposed to the closely packed samples). As shown in figure 5(a), the QW contains a small local widening. The electric potential developed by the applied gate voltage is

expected to be lower in the widened area. Electrons traveling across the QW would be backscattered due to mode mismatch resulting in effectively an attractive impurity in a QW. We estimate the additional depletion region extending from the gate edge to be 75–100 nm from other experiments. Therefore, the device is not expected to be a quantum dot and the argument is confirmed by the absence of the charging effect for $G < G_o$. In figures 5(b) and (c) of two cooling processes, only the first quantized plateau is sustained in the linear conductance. For $G > G_o$, conductance plateaus are distorted and missing. The fine structures of linear conductance are different by thermal cycling. The trace in figure 5(c) has several resonances while no resonance is in figure 5(b). The spectroscopy appears to be altered by thermal cycling and presents features of disordered QWs. In figure 5(d), double-splitting peaks are observable for $G < G_o$ and the ZBA is absent. The energy difference of splitting decreases with decreasing V_g. In contrast, the single-peak structure of ZBA is visible for $0.84G_o < G < G_o$ in figure 5(e). A conductance shoulder is present at $\sim 0.74G_o$ at zero bias and rises with increasing V_{sd}, becoming a resonant peak for $V_{sd} \gtrsim 0.88$ mV (crossings of traces). The deviations between two cooldowns are comprehensible by the fact that the ionized donors redistribute resulting in different averaged potential fluctuations which alter the impurity arrangements and correspondingly, the interference between the incident and backscattered electrons [17].

The ZBA is a peculiar phenomenon of QWs. The one-dimensional Kondo model which was based on the assumption of a spin-dependent localized potential was proposed to explain the experimental findings [27, 29–32]. Recently, Debray *et al* reported that a completely spin-polarized current can be generated by the asymmetrically lateral confinement for a high intrinsic spin–orbital coupling device [33]. Our device of low spin–orbital coupling is not in this catalog, and hence such asymmetric lateral spin–orbit coupling can be ignored. The ZBA was expected to split in parallel magnetic fields while the splitting width was about the Zeeman energy. However, several groups reported more intricate features of ZBA [24, 34, 28]. In some devices, splitting occurs in magnetic fields, but two split peaks can resolve back into a single peak by laterally shifting the QW. In some other devices, splitting even occurs in zero magnetic fields [28, 34]. Chen *et al* claimed that disorder is related to the splitting of the ZBA in magnetic fields [34]. Sarkozy *et al* and Lindelof *et al* suggested that resonant backscattering and length resonances could result in ZBA splitting [28, 35]. As we have demonstrated, impurities in QWs truly lead to such complicated features.

4. Conclusion

In conclusion, ZBA is robust in clean short QWs against lateral shifting and thermal cycling. On the other hand, impurities can cause resonances leading to the complicated source–drain spectroscopies. These resonant features are sensitive to thermal cycling and lateral shifting of QWs, revealing the random nature of impurities in ballistic QWs. The double-split peaks due to resonant levels affect the characteristics of ZBA. The results indicate that cleanliness (impurity-free) is crucial for studying the intrinsic behaviors of ZBA in one-dimensional systems.

Acknowledgments

We would like to thank C S Chu for useful discussions. This work was supported by the NSC grant in Taiwan under project no. NSC96-2112-M009-030-MY3 and the MOE ATU program.

References

[1] Wharam D A, Thornton T J, Newbury R, Pepper M, Ahmed H, Frost J E F, Hasko D G, Peacock D C, Ritchie D A and Jones G A C 1988 *J. Phys. C: Solid State Phys.* **21** L209
[2] van Wees B J, van Houten H, Beenakker C W J, Williamson J G, Kouwenhoven L P, van der Marel D and Foxon C T 1988 *Phys. Rev. Lett.* **60** 848
[3] van der Marel D and Haanappel E G 1989 *Phys. Rev.* B **39** 7811
[4] Chu C S and Sorbello R S 1989 *Phys. Rev.* B **40** 5941
[5] Nikolić K and MacKinnon A 1994 *Phys. Rev.* B **50** 11008
[6] Todorov T N and Briggs G A D 1994 *J. Phys.: Condens. Matter* **6** 2559
[7] Jura M P, Topinka M A, Urban L, Yazdani A, Shtrikman H, Pfeiffer L N, West K W and Goldhaber-Gordon D 2007 *Nat. Phys.* **3** 841
[8] McEuen P L, Alphenaar B W, Wheeler R G and Sacks R N 1990 *Surf. Sci.* **229** 312
[9] Tekman E and Ciraci S 1991 *Phys. Rev.* B **43** 7145
[10] Levinson Y B, Lubin M I and Sukhorukov E V 1992 *Phys. Rev.* B **45** 11936
[11] Gurvitz S A and Levinson Y B 1993 *Phys. Rev.* B **47** 10578
[12] Bardarson J H, Magnusdottir I, Gudmundsdottir G, Tang C S, Manolescu A and Gudmundsson V 2004 *Phys. Rev.* B **70** 245308
[13] Vargiamidis V and Polatoglou H M 2005 *Phys. Rev.* B **71** 075301
[14] Takagaki Y and Ferry D K 1992 *Phys. Rev.* B **46** 15218
[15] Mace D R, Grimshaw M P, Ritchie D A, Ford C J B, Pepper M and Jones G A C 1993 *J. Phys.: Condens. Matter* **5** L227
[16] Timp G L and Howard R E 1991 *Proc. IEEE* **79** 1188
[17] Nixon J A, Davies J H and Baranger H U 1991 *Phys. Rev.* B **43** 12638
[18] Brown R J, Kelly M J, Newbury R, Pepper M, Miller B, Ahmed H, Hasko D G, Peacock D C, Ritchie D A, Frost J E F and Jones G A C 1989 *Solid-State Electron.* **32** 1179
[19] Wakaya F, Takahara J, Takaoka S, Murase K and Gamo K 1996 *Japan. J. Appl. Phys.* **35** 1329
[20] Glazman L I and Larkin I A 1991 *Semicond. Sci. Technol.* **6** 32
[21] Cobden D H, Patel N K, Pepper M, Ritchie D A, Frost J E F and Jones G A C 1991 *Phys. Rev.* B **44** 1938
[22] Cobden D H, Savchenko A, Pepper M, Patel N K, Ritchie D A, Frost J E F and Jones G A C 1992 *Phys. Rev. Lett.* **69** 502
[23] Sakamoto T, Nakamura Y and Nakamura K 1995 *Appl. Phys. Lett.* **67** 2220
[24] Sfigakis F, Ford C J B, Pepper M, Kataoka M, Ritchie D A and Simmons M Y 2008 *Phys. Rev. Lett.* **100** 026807
[25] Thomas K J, Nicholls J T, Pepper M, Tribe W R, Simmons M Y and Ritchie D A 2000 *Phys. Rev.* B **61** R13365
[26] Liu K M, Umansky V and Hsu S Y 2010 *Phys. Rev.* B **81** 235316

[27] Cronenwett S M, Lynch H J, Goldhaber-Gordon D, Kouwenhoven L P, Marcus C M, Hirose K, Wingreen N S and Umansky V 2002 *Phys. Rev. Lett.* **88** 226805
[28] Sarkozy S, Sfigakis F, Das Gupta K, Farrer I, Ritchie D A, Jones G A C and Pepper M 2009 *Phys. Rev.* B **79** 161307
[29] Meir Y, Hirose K and Wingreen N S 2002 *Phys. Rev. Lett.* **89** 196802
[30] Hirose K, Meir Y and Wingreen N S 2003 *Phys. Rev. Lett.* **90** 026804
[31] Rejec T and Meir Y 2006 *Nature* **442** 900
[32] Hsiao J H, Liu K M, Hsu S Y and Hong T M 2009 *Phys. Rev.* B **79** 033304
[33] Debray P, Rahman S M S, Wan J, Nwerock R S, Cahay M, Ngo A T, Ulloa S E, Herbert S T, Muhammad M and Johnson M 2009 *Nat. Nanotechnol.* **4** 759
[34] Chen T M, Graham A C, Pepper M, Farrer I and Ritchie D A 2009 *Phys. Rev.* B **79** 153303
[35] Lindelof P E and Aagesen M 2008 *J. Phys.: Condens. Matter* **20** 164207